

Organic Polyradicals as Redox Mediators: Effect of Intramolecular Radical Interactions on Their Efficiency

Elena Badetti,^{*,○} Vega Lloveras,[○] Emanuele Amadio, Rosalia Di Lorenzo, Mara Olivares-Marín, Alvaro Y. Tesio, Songbai Zhang, Fangfang Pan, Kari Rissanen, Jaume Veciana, Dino Tonti,^{*} Jose Vidal-Gancedo,^{*} Cristiano Zonta, and Giulia Licini^{*}

Cite This: *ACS Appl. Mater. Interfaces* 2020, 12, 45968–45975

Read Online

ACCESS |

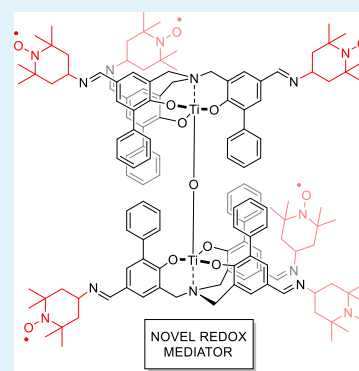
Metrics & More

Article Recommendations

Supporting Information

ABSTRACT: The spin–spin interactions between unpaired electrons in organic (poly)radicals, especially nitroxides, are largely investigated and are of crucial importance for their applications in areas such as organic magnetism, molecular charge transfer, or multiple spin labeling in structural biology. Recently, 2,2,6,6-tetramethylpiperidinyloxy and polymers functionalized with nitroxides have been described as successful redox mediators in several electrochemical applications; however, the study of spin–spin interaction effect in such an area is absent. This communication reports the preparation of a novel family of discrete polynitroxide molecules, with the same number of radical units but different arrangements to study the effect of intramolecular spin–spin interactions on their electrochemical potential and their use as oxidation redox mediators in a Li–oxygen battery. We find that the intensity of interactions, as measured by the d_1/d electron paramagnetic resonance parameter, progressively lowers the reduction potential. This allows us to tune the charging potential of the battery, optimizing its energy efficiency.

KEYWORDS: redox mediators, spin–spin interactions, TEMPO, nitroxides, μ -oxo complexes, titanatranes



INTRODUCTION

The spin–spin interactions between unpaired electrons in organic diradicals and polyradicals are of crucial importance in many areas such as organic magnetism,^{1–5} molecular charge transfer,⁶ or multiple spin labeling in structural biology.⁷ When unpaired electrons are in close proximity, the dominant interaction is likely to be spin-exchange coupling and dipole–dipole interactions. The origin of such radical–radical interactions could be intra- and/or intermolecular, that is, between radicals of the same molecule or radicals from different species. Intramolecular interactions exist when radical units within a structure are close enough and are detected at both low and high concentrations, whereas intermolecular interactions exist only at high concentrations because of the higher proximity between molecules. Among organic radicals, nitroxides have the advantage of being stable under ambient conditions and can be easily synthesized, functionalized, and manipulated. Di- and polynitroxides have shown improved properties with respect to mononitroxides as organic ferromagnets, labels in electron magnetic resonance imaging, radiation protectors during whole brain radiotherapy, or as polarizing agents in dynamic nuclear polarization (DNP).⁸ For example, when used as electron spin agents for DNP, dinitroxides can enhance the sensitivity of nuclear magnetic resonance signals by orders of magnitude compared with mononitroxides. Among other factors, the intramolecular exchange interactions and electron–electron dipolar coupling

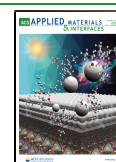
are the possible spin relaxation enhancement pathways.^{9–11} We are not aware of the effects reported beyond magnetic properties. Nitroxide radicals also have relevant electrochemical properties and have been used as redox charge mediators.

Redox mediation is a mechanism ubiquitous in nature, used to transport electrons in solution phase, usually to connect a catalytic center to another one or to a reactant. In general, the redox mediator (RM) is a soluble component able to exchange an electron with a redox center, to diffuse to a different redox center, and to exchange again an electron to restore its initial state. In the cell respiratory system, for example, nicotinamide adenine dinucleotide hydrogen (NADH) shuttles electrons through the membrane, and three distinct complexes are involved in the electron transport chain in the mitochondria before reducing oxygen to water.^{12,13} In photosynthesis, different quinones play similar roles between the reactive complexes involved.¹⁴ In part, inspired by such systems, several chemical and electrochemical energy conversion or storage

Received: June 25, 2020

Accepted: September 15, 2020

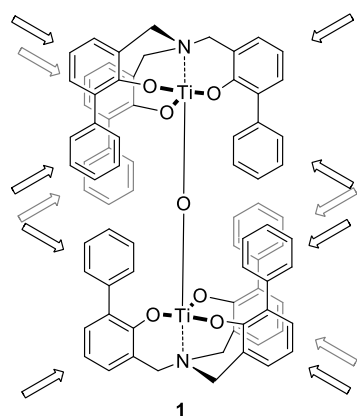
Published: September 15, 2020



systems rely or are improved by the use of RMs (i.e., artificial photosynthesis, organic dye-sensitized solar cells, pseudocapacitors, and redox flow, lithium–sulfur, and metal–oxygen batteries).¹⁵ Nitroxides, in particular, 2,2,6,6-tetramethylpiperidinyloxy (TEMPO) monoradical, have been widely studied in the past two decades in energy storage,^{16,17} either as part of the cathode¹⁸ or in the electrolyte.¹⁹ Being part of the cathode, TEMPO could be used, for instance, as an active material in an organic-based paper battery²⁰ or to tune conductivity in a conjugated radical polymer battery.^{21,22} On the other hand, it could be used in the electrolyte as a catholyte for redox flow batteries²³ or as a soluble oxidation mediator in metal–oxygen batteries.²⁴ This wide use is due to its appropriate potential, kinetics, and availability.²⁵ Some polynitroxide compounds, such as polymers functionalized with nitroxides, have been described exhibiting a high mediation of charge.^{26,27}

The aim of this study is to functionalize the molecules in Scheme 1 to obtain a polynitroxide. To the best of our

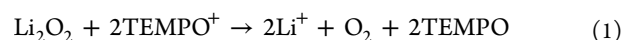
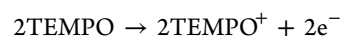
Scheme 1. Reported μ -Oxo Dinuclear Titanium Complex I with the Possible Functionalization Indicated



knowledge, mediation has not been reported with discrete molecules presenting several identical (nitroxides) redox centers with a well-defined arrangement, and the effect of intramolecular radical interactions still remains a challenging mechanism to understand. In addition, a comparison between polynitroxides and mononitroxides is also absent. The intensity of the intramolecular spin–spin interactions increases mainly with the proximity of the radical units and the number of interacting radicals and can be detected and studied by

electron paramagnetic resonance (EPR) spectroscopy.^{28,29} In this work, we study the effect of intramolecular spin–spin interactions in polynitroxide molecules on their electrochemical potential and their use as RMs, in particular as charge mediators in aprotic lithium–oxygen batteries. These batteries present high theoretical capacities because of the reaction between pure lightweight elements (Li and O₂) and the solid product (Li₂O₂) but are affected by several issues related to the formation of reactive intermediates and passivation by Li₂O₂.³⁰

Mediators are critical in two different processes of metal–air batteries: they allow to delay electrode passivation during discharge and assist peroxide removal during charge.^{31,32} Using mediators with the redox potential below the oxygen reduction potential ($E^0 = 2.96$ V vs Li/Li⁺) results in an oxygen reduction reaction (ORR) with enhanced kinetics and discharge capacity.^{33–36} Instead, when its redox potential is above the equilibrium potential, the mediator is active during charge, where it is oxidized at the electrode, diffuses to Li₂O₂, with which it chemically reacts to give place to oxygen evolution (oxygen evolution reaction OER).^{24,31,37–40} Thus, in the case of TEMPO nitroxide, we have the following catalytic scheme

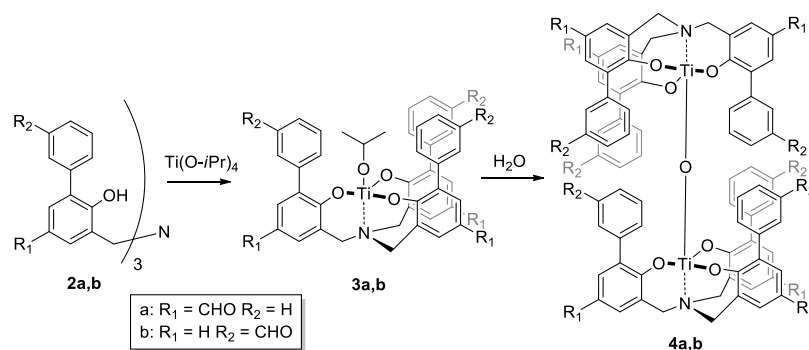


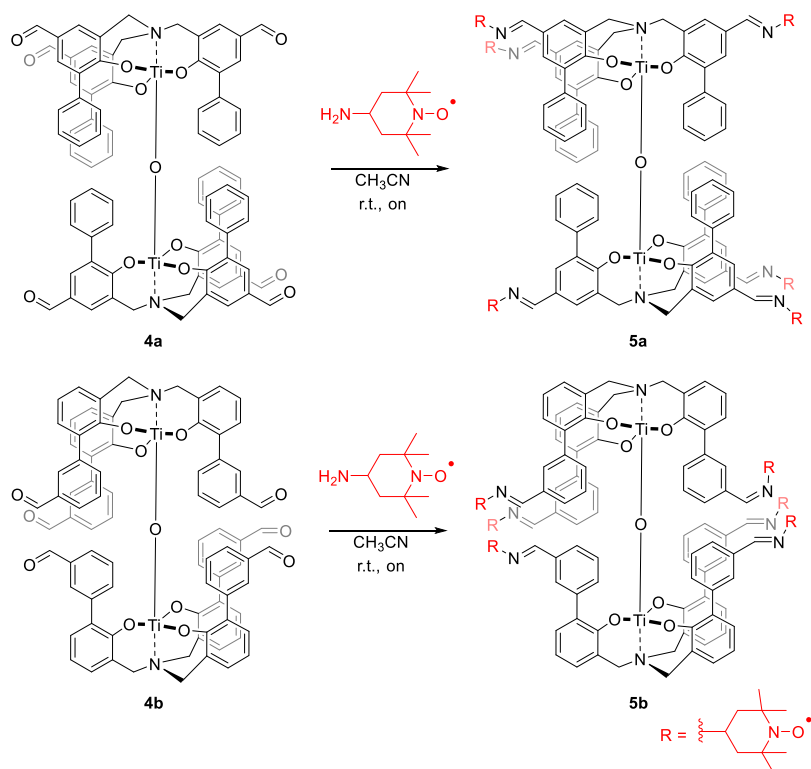
For efficient operation, apart from the appropriate reduction potential, a mediator requires stability in cell components and intermediates,³⁹ reactivity with Li₂O₂,⁴¹ and moderate diffusivity.³² The latter is necessary to minimize shuttling to the anode and is favored by larger compounds, whereas nitroxides are regarded as one of the most stable functional groups among halogenides, quinones, and several other organic molecules.⁴²

To obtain the target molecules, the aim of the present study, we have used as scaffold triphenolamines,⁴³ in particular a μ -oxo dinuclear titanium complex I (Scheme 1).⁴⁴

In recent years, we reported about the use of tetradentate metal complexes,^{45–48} molecular recognition,^{49–54} and as molecular scaffolds for multiple functionalization. Among the different structures, μ -oxo dinuclear titanium complex I represents the ideal architecture to become a scaffold for multiple functionalization (Scheme 1). This system, which spontaneously forms starting from two titanatranes units via selective hydrolysis, has a well-defined geometry, and it is stable even in the presence of water. The

Scheme 2. μ -Oxo Complexes 4a–b can be Obtained from the Corresponding Phenol Derivatives 2a–b by Reaction with Ti(O-*i*Pr)₄; the Mononuclear Titanatranes Systems 3a–b Evolve Spontaneously to the Corresponding 4a–b in the Presence of Traces of water



Scheme 3. Synthesis of TEMPO-Functionalized Dinuclear μ -Oxo Titanium (IV) Complexes 5a–b

overall stability, combined by the defined geometry, makes this molecular structure ideal for multiple functionalization with RMs.

In the present paper, we report about: (i) the synthetic evolution of the system in order to obtain a molecular scaffold suitable for multiple functionalization, (ii) the preparation of defined molecular systems containing the same number of radical units with different arrangements, some with closer and others with more distant radical dispositions, (iii) the study of the intramolecular interaction strength among radicals in the different arrangements, and (iv) the effect of such radical interactions on their electrochemical behavior and RM capabilities.

RESULTS AND DISCUSSION

Synthesis of Multiple Radical Molecular Architectures. As shown in our previous paper, titanatranes with bulky phenyl substituents in ortho positions spontaneously form highly stable μ -oxo dinuclear complexes in the presence of traces of water.⁴⁴ We took advantage of this chemistry to synthesize a series of novel μ -oxo complexes **4a–b**, bearing aldehydes in different positions (Scheme 2). Aldehydes were chosen as possible anchoring points for the subsequent introduction of amino-TEMPO units via the imine condensation reaction. The parent ligands **2a–b** were prepared with a newly developed synthesis method (see Supporting Information, Chapter S1).

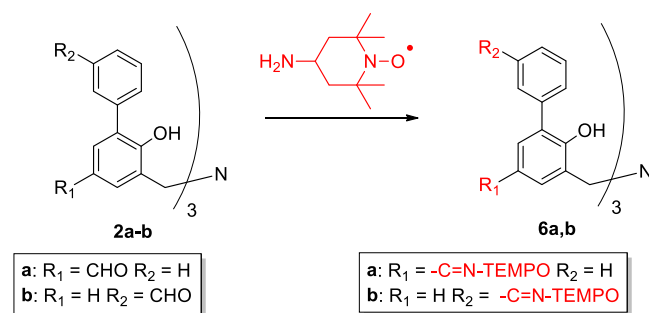
This takes advantage of either a direct threefold formylation of a preformed ligand, for the functionalization of the phenol para positions (*viz.* **2a**), or a Suzuki coupling with formyl-arylboronic acid for the functionalization of the upper substituted phenyl ring (*viz.* **2b**). The reaction between the amine triphenolates **2a–b** and $\text{Ti}(\text{O}-i\text{Pr})_4$ resulted in the *in situ* formation of the C_3 mononuclear $\text{Ti}(\text{IV})$ complexes **3a–b**

which rapidly and spontaneously self-assemble, in the presence of traces of water, into the dinuclear μ -oxo **4a–b**, as the only S_6 -symmetric system (Scheme 2). The complexation and formation of the dinuclear μ -oxo titanium (IV) complexes can be easily followed by ^1H NMR spectroscopy. As an example, by the addition of 1 equiv of $\text{Ti}(\text{O}-i\text{Pr})_4$ to **2b**, the ^1H NMR spectrum in CDCl_3 shows the formation of a single set of signals at 3.69 ppm for the methylene protons α to the nitrogen of **3b** (see Supporting Information Figure S12). Upon the addition of few amount of water, **3b** rapidly evolves into the dinuclear μ -oxo complex **4b**, which precipitates over time from the solution. The ^1H NMR spectrum of **4b** shows the formation of an AB system at 4.40 and 3.31 ppm, corresponding to the methylene protons (see Supporting Information Figure S13). Moreover, the aromatic protons of the peripheral aryl rings, together with the aldehydic signal, are shifted upfield (for CHO, from 9.94 to 9.20 ppm) because of the intercalation of the rings around the μ -oxo bridge. The formation of the dimeric complexes **4a–b** is also confirmed by electrospray ionization-mass spectrometry (ESI-MS) analysis. As an example, for **4b**, the spectra, both in the positive and negative modes, clearly display the characteristic isotopic distribution for the formation of $[\text{M}]^-$ ($m/z = 1041.2$) or of the complex having Na^+ counterion ($m/z = 1423.4$).

Condensation between **4a–b** and the radical 4-amino-TEMPO has allowed to obtain compounds **5a–b** (Scheme 3). The handling of radicals in solution was carried out under dark and anhydrous conditions to avoid, respectively, the possible degradation of the radicals and imine bond hydrolysis. This postfunctionalization leads to the construction of stable and spatially ordered structures with multiple mediator functionalities disposed in a controlled way into space. Similarly, to have a comparison with a less spatially defined system, radical carriers **6a–b** were prepared starting from ligands **2a–b**

(Scheme 4). The novel μ -oxo complexes **5a–b** and ligands **6a–b** were characterized by ESI-MS, Fourier transform

Scheme 4. Synthesis of TEMPO-Functionalized Ligands 6a–b



infrared (FTIR) spectroscopy, elemental analysis, and EPR spectroscopy. In the ESI-MS spectra, all experimental isotopic clusters were in agreement with the theoretical ones. The FTIR measurements for all the systems showed the disappearance of the characteristic carbonyl stretching of the aldehyde (at *ca.* 1700 cm^{-1}) and the appearance of the stretching peak of the C=N bond (at *ca.* 1600 cm^{-1}). The full functionalization with the radicals of all compounds was quantitatively determined by EPR spectroscopy (see Supporting Information Table S1).

The X-ray structure of **5b** unambiguously confirmed the dimer formation as well as the condensation between the radical 4-amino-TEMPO and the aldehyde moieties present in **4b** (Figure 1). The molecular structure of this radical-functionalized dinuclear system **5b** shows a C_3 symmetry in

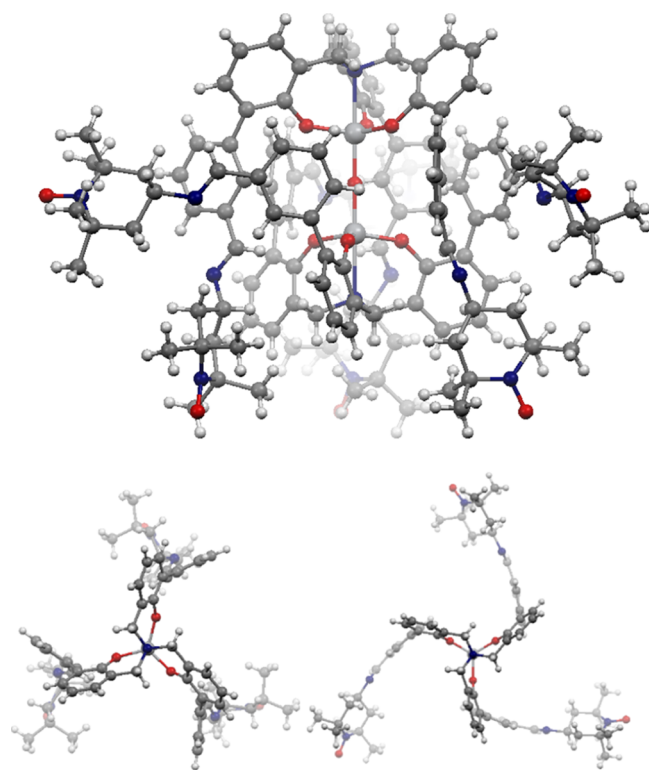


Figure 1. X-ray single crystal structure of **5b** and details of the relative orientations of the two titanatrane units in the μ -oxo system.

the solid state instead of the S_6 -symmetric system in solution that was observed for **4b**.

Ligands **6a–b** and the corresponding μ -oxo complexes **5a–b** were investigated by EPR to gather information on the relative arrangement of the radicals in solution. The results obtained were then correlated to their electrochemical properties evaluated by cyclic voltammetry and finally to the OER RMs for Li–O₂ batteries. The same concentration has been used in each pair.

EPR Spectroscopy for Polyradical Species 5a–b and 6a–b. The EPR study was done in diluted conditions to focus on intramolecular radical interactions. The EPR spectra of the polyradical species at 300 K (Figure 2) showed mainly a three-

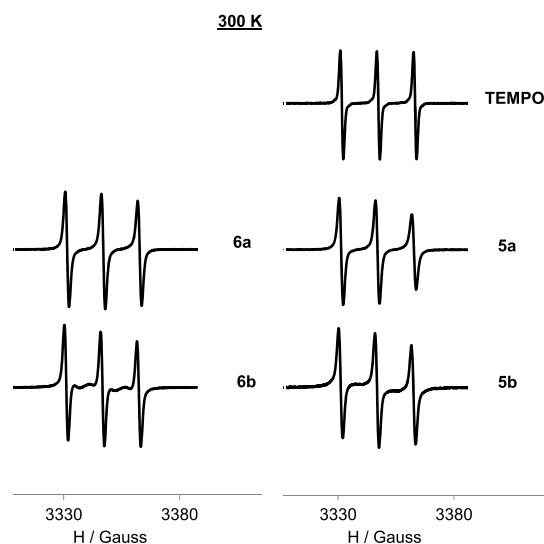


Figure 2. Normalized EPR spectra of TEMPO, ligands **6a–6b**, and μ -oxo complexes **5a–5b** in DCM/toluene 1:1, at 300 K and 1 mM.

line pattern like that of the TEMPO free radical, although with broader lines and a selective decrease of the high-field line because of the hindered motion of the radicals attached to a big molecule. In addition, some signs related to the radical interactions were observed. In the EPR spectra of the corresponding **b** species (**6b** and **5b**), some little alternating linewidth effect compared with their respective **a** species (**6a** and **5a**) was observed. This means some spin-exchange interaction among the radicals in such compounds. In fact, the radicals in **b** conformations present more degrees of freedom than in **a**, favoring their mobility and hence their proximity.

In a frozen solution, 120 K, the EPR spectral shape changes completely. Under these anisotropic conditions, the spectral shape is sensitive to the distance between neighboring nitroxides up to *ca.* 2 nm, and a convenient measure of the strength of the dipole–dipole interactions is therefore given by the empirical ratio of peak heights, the d_1/d value (Figure 3).⁵⁵ The higher the ratio, the shorter the distance between the radical centers, and hence the higher the radical interactions. Table 1 displays the calculated d_1/d values for all compounds from their corresponding frozen solution spectra (shown in Figures 3 and Supporting Information S15–S16). The d_1/d ratio was 0.51 for the monoradical TEMPO where intramolecular interactions are absent, whereas for all the polyradical species, this ratio was much higher. This suggested that all of them presented intramolecular dipolar interactions

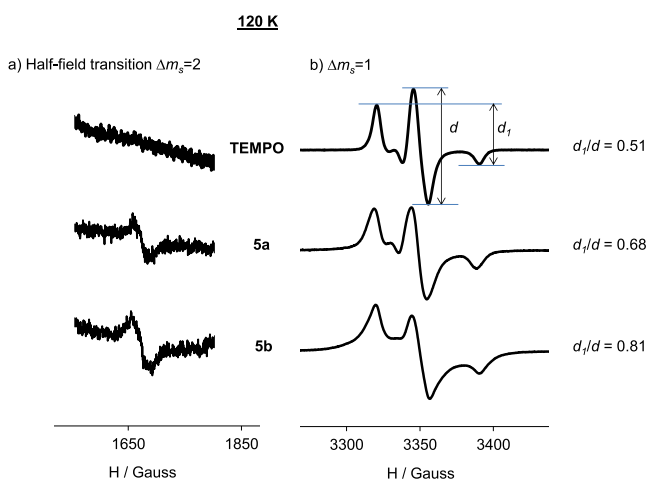


Figure 3. (a) $|\Delta m_s| = 2$ transition at half-field EPR spectra and (b) $|\Delta m_s| = 1$ EPR spectra of TEMPO and μ -oxo complexes **5a–5b** in DCM/toluene 1:1 at 120 K and 1 mM.

Table 1. EPR and Electrochemical Parameters of Compounds **5a–b** and **6a–b**^a

	d_1/d	$ \Delta m_s = 2$ intensity	$E_{1/2}$ (V) vs Ag/AgCl	voltage (V) vs Li^+/Li at 0.05 mA/cm ²
6a	0.69	1.0	0.86	3.94
6b	0.85	1.05	0.84	3.83
5a	0.68	1.3	0.86	3.89
5b	0.81	1.6	0.83	3.81

^aMeasure replicates show variations in the range of ± 2 mV for $E_{1/2}$ and ± 0001 for d_1/d .

and that some of their radicals should be located at distances lower than 2 nm. This compares well with the 7.846 Å radical–radical distance found in the crystal structure. In detail, both in the ligands and μ -oxo complex pairs, higher d_1/d values, that is, closer radicals, in their corresponding **b** arrangement (0.85 and 0.81 for **6b** and **5b** as against 0.69 and 0.68 for **6a** and **5a**, respectively) were observed. In addition, under these conditions, all polyradical compounds showed a half-field transition of $|\Delta m_s| = 2$. This signal is characteristic of dipolar coupled spins and a direct evidence of the presence of a high-spin state. It is mainly generated by the presence of two radical units closer than a critical distance, and its intensity depends on the average distance between them and the number of interacting pairs of radicals. Therefore, the half-field signal intensity was used as a second independent parameter to quantify the radical interactions in our compounds. In Table 1 are also reported the normalized half-field signal intensities of all compounds, and in Figures 3 (and Supporting Information S17), their corresponding EPR spectra.

Following the same trend, the half-field intensity was also larger in the **b** species. This difference in intensity is significant in the μ -oxo complex pair (**5a** vs **5b**) and can be explained taking into account the different locations of the radicals in the scaffold. In **5b**, the radicals of both titanatranes are disposed in closer proximity than in **5a**. In fact, the **5b** X-ray structure displays three close enough (7.846 Å) pairs of radicals (each pair with the radicals of both titanatranes). The corresponding EPR study of the TEMPO free radical in frozen solution is explained in the Supporting Information.

Cyclic Voltammeteries of Compounds 5a–b and 6a–b. The electrochemical properties of the polyradical species under

study and the TEMPO free radical were evaluated by cyclic voltammetry (CV) in DMF, with 0.1 M of tetrabutylammonium hexafluorophosphate (TBAHFP) as the electrolyte. The corresponding cyclic voltammograms are shown in Figure 4

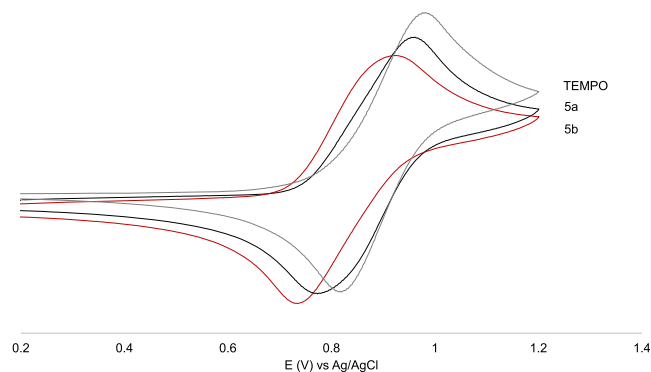


Figure 4. Cyclic voltammetry of TEMPO and μ -oxo complexes **5a–5b** at 1 mM in DMF with 0.1 M TBAHFP vs Ag/AgCl at the scan rate of 200 mV/s.

(see also Supporting Information Figure S18–S20 and Figure S21 for CV at different scan rates), and the half-wave potential values $E_{1/2}$ are included in Table 1. The polyradical compounds exhibited a reversible redox wave at lower potential values than the monoradical TEMPO ($E_{1/2} = -0.9$ V, see Supporting Information Table S2). Focusing on the different polynitroxides, it can be observed that the **b** species (**6b** and **5b**) exhibited lower $E_{1/2}$ potential than their corresponding homologues with the **a** arrangement (**6a** and **5a**, respectively). These relations are a clear indication of the mutual interactions between the redox centers existing in these polyradical species (absent in the monoradical TEMPO) and can be explained by means of intramolecular electron–electron interaction effects. As previously reported,⁵⁶ in the polyradical species with a closer radical disposition (higher interactions), this shift was higher. As shown in Figure 5 we observe an interesting correlation between the $E_{1/2}$ potential and the d_1/d parameter. This suggests that the same interactions caused by the close distance forced by the ligand geometry on one hand are reflected in the magnetic radical coupling, and on the other

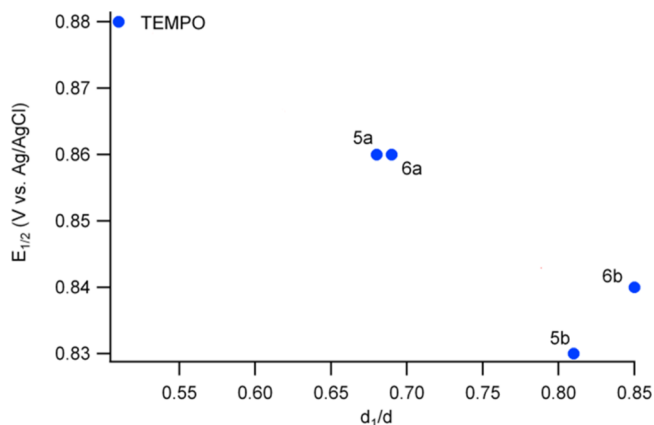


Figure 5. Half-wave potential $E_{1/2}$ vs d_1/d of TEMPO and polynitroxides **6a–b** and **5a–b** at the same molecular concentration of 1 mM.

hand destabilize the electronic level of the radical state, resulting in a lower reduction potential.

Compounds 5a–b and 6a–b as Redox Charge Mediators. Ligands 6a–b and their corresponding μ -oxo complexes (5a–b) were tested as redox charge mediators for Li–O₂ batteries. Typical galvanostatic discharge and charge profiles are reported in Figure 6 (see also Supporting

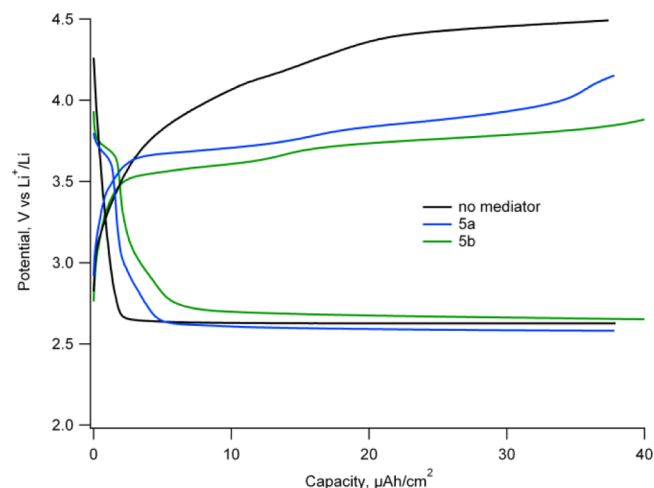


Figure 6. Charge and discharge galvanostatic pulses with the electrolyte without additives and using 5a–b mediators at 1 mM at current densities of 0.05 mA/cm².

Information Figure S22 for the complete dataset and the corresponding polarization curves). Table 1 reports their corresponding cell voltages versus Li⁺/Li when a charging current of 0.05 mA/cm² was applied. Compared to the electrolyte without additives, we clearly observe mediation of charge, with general tendencies consistent with the potential shifts obtained by cyclic voltammetry, as graphically also shown in Figure S24. This implies that the larger molecular size does not affect the mediation activity as much as the redox potential.

Remarkably, we can observe that by using TEMPO mononitroxide at different concentrations, from 1 to 12 mM, we measured systematically higher charge voltages than those obtained with the polynitroxide species under study (Supporting Information Figure S23 and Tables S2–S3). Although there was a tendency toward lower charge voltage by increasing the TEMPO radical concentration, which was also reported elsewhere,²⁵ even at double radical concentration than polynitroxides (12 mM), the TEMPO charge voltage was still higher (see Supporting Information Table S2). In addition, the charge potential decreases from 6a to 5b, much more than the corresponding $E_{1/2}$ variation even if the same radical concentration has been used. This suggests that intramolecular interactions also have a direct impact on the kinetic efficiency of polynitroxides as charge mediators, which sums to the thermodynamic variation of redox potential.

CONCLUSIONS

Triphenolamines and μ -oxo dinuclear Ti(IV) complexes with versatile multiple functionalization and a well-defined geometry have been synthesized and characterized. These molecular scaffolds have permitted us to anchor up to six redox-active TEMPO radical units in two different arrangements (some with closer and others with more distant radical dispositions)

to study the influence of the intramolecular radical interactions on their electrochemical and OER mediator behavior. These polyradical species have been synthesized and characterized. We studied by EPR and X-ray diffraction the arrangement of the radical units in such molecular scaffolds, and their mutual interactions, and quantified their electrochemical behavior by cyclic voltammetry and their radical efficiency as RM, by the charge voltage in a Li/O₂ battery.

We conclude that multiple TEMPO redox units in the same discrete molecular scaffold can favor the efficiency as OER mediator compared with monoradical species. In particular, the better performances observed are related to the closer disposition of the radical units and the higher number of pairs of radicals that can interact intramolecularly. Such intramolecular interactions seem to decrease the half-wave potential of the electroactive TEMPO radical units. In a Li–O₂ battery, this allows to tune the charging potential toward lower values, making more efficient the OER RM process. In fact, the smaller difference between the discharge and charge potential increases the energy efficiency, and the lower overpotential decreases the probability of secondary reactions. Thus, this study suggests a correlation between the radical efficiency as RM and the intramolecular radical interactions quantified by EPR. Further studies are in progress to evaluate such effects with a bigger family of polynitroxide systems.

ASSOCIATED CONTENT

Supporting Information

The Supporting Information is available free of charge at <https://pubs.acs.org/doi/10.1021/acsami.0c09386>.

Compound synthesis and characterization, EPR, and charge and discharge galvanostatic pulses (PDF)

AUTHOR INFORMATION

Corresponding Authors

Elena Badetti – Department of Chemical Sciences and CIRCC Padova Unit, University of Padova, 35131 Padova, Italy; orcid.org/0000-0002-3984-7829; Email: elena.badetti@unive.it

Dino Tonti – Institut de Ciència de Materials de Barcelona (ICMAB-CSIC), E-08193 Cerdanyola del Valles, Spain; orcid.org/0000-0003-0240-1011; Email: dino.t@csic.es

Jose Vidal-Gancedo – Institut de Ciència de Materials de Barcelona (ICMAB-CSIC), E-08193 Cerdanyola del Valles, Spain; Networking Research Center on Bioengineering, Biomaterials and Nanomedicine (CIBER-BBN), E-08193 Barcelona, Spain; orcid.org/0000-0002-1853-9675; Email: j.vidal@icmab.es

Giulia Licini – Department of Chemical Sciences and CIRCC Padova Unit, University of Padova, 35131 Padova, Italy; orcid.org/0000-0001-8304-0443; Email: giulia.licini@unipd.it

Authors

Vega Lloveras – Institut de Ciència de Materials de Barcelona (ICMAB-CSIC), E-08193 Cerdanyola del Valles, Spain; Networking Research Center on Bioengineering, Biomaterials and Nanomedicine (CIBER-BBN), E-08193 Barcelona, Spain; orcid.org/0000-0002-9653-3340

Emanuele Amadio – Department of Chemical Sciences and CIRCC Padova Unit, University of Padova, 35131 Padova, Italy; orcid.org/0000-0001-7736-5946

Rosalia Di Lorenzo – Department of Chemical Sciences and CIRCC Padova Unit, University of Padova, 35131 Padova, Italy

Mara Olivares-Marín – Institut de Ciència de Materials de Barcelona (ICMAB-CSIC), E-08193 Cerdanyola del Valles, Spain; Department of Mechanical, Energy and Materials Engineering, University Centre of Mérida, University of Extremadura, 06800 Mérida, Spain

Alvaro Y. Tesio – Institut de Ciència de Materials de Barcelona (ICMAB-CSIC), E-08193 Cerdanyola del Valles, Spain; Centro de Investigación y Desarrollo en Materiales Avanzados y Almacenamiento de Energía de Jujuy (CIDMEJu), Centro de Desarrollo Tecnológico General Manuel Savio, Palpalá Y 4612, Jujuy, Argentina; orcid.org/0000-0001-9004-5947

Songbai Zhang – Institut de Ciència de Materials de Barcelona (ICMAB-CSIC), E-08193 Cerdanyola del Valles, Spain; orcid.org/0000-0003-1084-6483

Fangfang Pan – Department of Chemistry, University of Jyväskylä, 40014 Jyväskylä, Finland; orcid.org/0000-0002-3091-6795

Kari Rissanen – Department of Chemistry, University of Jyväskylä, 40014 Jyväskylä, Finland; orcid.org/0000-0002-7282-8419

Jaume Veciana – Institut de Ciència de Materials de Barcelona (ICMAB-CSIC), E-08193 Cerdanyola del Valles, Spain; Networking Research Center on Bioengineering, Biomaterials and Nanomedicine (CIBER-BBN), E-08193 Barcelona, Spain; orcid.org/0000-0003-1023-9923

Cristiano Zonta – Department of Chemical Sciences and CIRCC Padova Unit, University of Padova, 35131 Padova, Italy; orcid.org/0000-0003-1749-7482

Complete contact information is available at: <https://pubs.acs.org/10.1021/acsami.0c09386>

Author Contributions

[○]E.B. and V.L. contributed equally to the work.

Notes

The authors declare no competing financial interest.

ACKNOWLEDGMENTS

This work was supported by: DGICT-MINECO (MAT2016-80826-R, MAT2017-91404-EXP, RTI2018-09273-B-I00), AGAUR (2017 SGR 918, 2014 SGR 1505, 2017 SGR 1687) and University of Padova. ICMAB acknowledges Spanish MINECO through the Severo Ochoa Centres of Excellence Programme Grant SEV- 2015-0496 and S.Z. his CSC grant.

REFERENCES

- (1) Iwamura, H.; Koga, N. Studies of Organic Di-, Oligo-, and Polyradicals by Means of Their Bulk Magnetic Properties. *Acc. Chem. Res.* **1993**, *26*, 346–351.
- (2) Rajca, A. The Physical Organic Chemistry of Very High-Spin Polyradicals. *Advances in Physical Organic Chemistry* **2005**, *40*, 153.
- (3) Rajca, A.; Wongsriratanakul, J.; Rajca, S. Magnetic Ordering in an Organic Polymer. *Science* **2001**, *294*, 1503–1505.
- (4) Rajca, A.; Shiraishi, K.; Vale, M.; Han, H.; Rajca, S. Stable Hydrocarbon Diradical, An Analogue of Trimethylenemethane. *J. Am. Chem. Soc.* **2005**, *127*, 9014–9020.
- (5) Fukuzaki, E.; Nishide, H. Room-Temperature High-Spin Organic Single Molecule: Nanometer-Sized and Hyperbranched Poly[1,2,(4)-phenylenevinyleneanisylaminium]. *J. Am. Chem. Soc.* **2006**, *128*, 996–1001.

(6) Chernick, E. T.; Mi, Q.; Kelley, R. F.; Weiss, E. A.; Jones, B. A.; Marks, T. J.; Ratner, M. A.; Wasielewski, M. R. Electron Donor–Bridge–Acceptor Molecules with Bridging Nitronyl Nitroxide Radicals: Influence of a Third Spin on Charge- and Spin-Transfer Dynamics. *J. Am. Chem. Soc.* **2006**, *128*, 4356–4364.

(7) Altenbach, C.; Oh, K.-J.; Trabanino, R. J.; Hideg, K.; Hubbell, W. L. Estimation of Inter-Residue Distances in Spin Labeled Proteins at Physiological Temperatures: Experimental Strategies and Practical Limitations†. *Biochemistry* **2001**, *40*, 15471–15482.

(8) Huang, L.; Yan, C.; Cui, D.; Yan, Y.; Liu, X.; Lu, X.; Tan, X.; Lu, X.; Xu, J.; Xu, Y.; Liu, R. Organic Radical Contrast Agents Based on Polyacetylenes Containing 2,2,6,6-Tetramethylpiperidine 1-Oxyl (TEMPO): Targeted Magnetic Resonance (MR)/Optical Bimodal Imaging of Folate Receptor Expressing HeLa Tumors in Vitro and in Vivo. *Macromol. Biosci.* **2015**, *15*, 788–798.

(9) Matsuki, Y.; Maly, T.; Ouari, O.; Karoui, H.; Le Moigne, F.; Rizzato, E.; Lyubenova, S.; Herzfeld, J.; Prisner, T.; Tordo, P.; Griffin, R. G. Dynamic Nuclear Polarization with a Rigid Biradical. *Angew. Chem. Int. Ed.* **2009**, *48*, 4996–5000.

(10) Song, C.; Hu, K.-N.; Joo, C.-G.; Swager, T. M.; Griffin, R. G. TOTAPOL: A Biradical Polarizing Agent for Dynamic Nuclear Polarization Experiments in Aqueous Media. *J. Am. Chem. Soc.* **2006**, *128*, 11385–11390.

(11) Pinto, L. F.; Marín-Montesinos, I.; Lloveras, V.; Muñoz-Gómez, J. L.; Pons, M.; Veciana, J.; Vidal-Gancedo, J. NMR signal enhancement of >50 000 times in fast dissolution dynamic nuclear polarization. *Chem. Commun.* **2017**, *53*, 3757–3760.

(12) Green, D. E.; Tzagoloff, A. The Mitochondrial Electron Transfer Chain. *Arch. Biochem. Biophys.* **1966**, *116*, 293–304.

(13) Kracke, F.; Vassilev, I.; Krömer, J. O. Microbial electron transport and energy conservation - the foundation for optimizing bioelectrochemical systems. *Front. Microbiol.* **2015**, *6*, 575.

(14) Crofts, A. R.; Wraight, C. A. The Electrochemical Domain of Photosynthesis. *Biochim. Biophys. Acta Rev. Bioenerg.* **1983**, *726*, 149–185.

(15) Boschloo, G.; Hagfeldt, A. Characteristics of the Iodide/Triiodide Redox Mediator in Dye-Sensitized Solar Cells. *Acc. Chem. Res.* **2009**, *42*, 1819–1826.

(16) Kim, J.; Kim, J. H.; Ariga, K. Redox-Active Polymers for Energy Storage Nanoarchitectonics. *Joule* **2017**, *1*, 739–768.

(17) Friebe, C.; Lex-Balducci, A.; Schubert, U. S. Sustainable Energy Storage: Recent Trends and Developments toward Fully Organic Batteries. *ChemSusChem* **2019**, *12*, 4093–4115.

(18) Xie, Y.; Zhang, K.; Monteiro, M. J.; Jia, Z. Conjugated Nitroxide Radical Polymers: Synthesis and Application in Flexible Energy Storage Devices. *ACS Appl. Mater. Interfaces* **2019**, *11*, 7096–7103.

(19) Lai, Y. Y.; Li, X.; Zhu, Y. Polymeric Active Materials for Redox Flow Battery Application. *ACS Appl. Polym. Mater.* **2020**, *2*, 113–128.

(20) Suga, T.; Konishi, H.; Nishide, H. Photocrosslinked Nitroxide Polymer Cathode-Active Materials for Application in an Organic-Based Paper Battery. *Chem. Commun.* **2007**, 1730–1732.

(21) Li, F.; Wang, S.; Zhang, Y.; Lutkenhaus, J. L. Electrochemical Energy Storage in Poly(Dithieno[3,2-b:2',3'-d]Pyrrole) Bearing Pendant Nitroxide Radicals. *Chem. Mater.* **2018**, *30*, 5169–5174.

(22) Wang, S.; Li, F.; Easley, A. D.; Lutkenhaus, J. L. Real-Time Insight into the Doping Mechanism of Redox-Active Organic Radical Polymers. *Nat. Mater.* **2019**, *18*, 69–75.

(23) Wei, X.; Xu, W.; Vijayakumar, M.; Cosimbescu, L.; Liu, T.; Sprenkle, V.; Wang, W. TEMPO-Based Catholyte for High-Energy Density Nonaqueous Redox Flow Batteries. *Adv. Mater.* **2014**, *26*, 7649–7653.

(24) Bergner, B. J.; Schürmann, A.; Peppler, K.; Garsuch, A.; Janek, J. TEMPO: A Mobile Catalyst for Rechargeable Li-O₂ Batteries. *J. Am. Chem. Soc.* **2014**, *136*, 15054–15064.

(25) Bergner, B. J.; Hofmann, C.; Schürmann, A.; Schröder, D.; Peppler, K.; Schreiner, P. R.; Janek, J. Understanding the Fundamentals of Redox Mediators in Li–O₂ Batteries: A Case

Study on Nitroxides. *Phys. Chem. Chem. Phys.* **2015**, *17*, 31769–31779.

(26) Vlad, A.; Rolland, J.; Hauffman, G.; Ernould, B.; Gohy, J.-F. Melt-Polymerization of TEMPO Methacrylates with Nano Carbons Enables Superior Battery Materials. *ChemSusChem* **2015**, *8*, 1692–1696.

(27) Nishide, H.; Iwasa, S.; Pu, Y.-J.; Suga, T.; Nakahara, K.; Satoh, M. Organic radical battery: nitroxide polymers as a cathode-active material. *Electrochim. Acta* **2004**, *50*, 827–831.

(28) Badetti, E.; Lloveras, V.; Muñoz-Gómez, J. L.; Sebastián, R. M.; Caminade, A. M.; Majoral, J. P.; Veciana, J.; Vidal-Gancedo, J. Radical Dendrimers: A Family of Five Generations of Phosphorus Dendrimers Functionalized with TEMPO Radicals. *Macromolecules* **2014**, *47*, 7717–7724.

(29) Badetti, E.; Lloveras, V.; Scaramuzzo, F. A.; Wurst, K.; Veciana, J.; Vidal-Gancedo, J.; Licini, G.; Zonta, C. Tris-Pyridylmethylamine (TPMA) Complexes Functionalized with Persistent Nitronyl Nitroxide Organic Radicals. *Dalton Trans.* **2020**, *49*, 10011–10016.

(30) Christensen, J.; Albertus, P.; Sanchez-Carrera, R. S.; Lohmann, T.; Kozinsky, B.; Liedtke, R.; Ahmed, J.; Kojic, A. A Critical Review of Li/Air Batteries. *J. Electrochem. Soc.* **2011**, *159*, R1–R30.

(31) Lim, H.-D.; Lee, B.; Zheng, Y.; Hong, J.; Kim, J.; Gwon, H.; Ko, Y.; Lee, M.; Cho, K.; Kang, K. Rational Design of Redox Mediators for Advanced Li-O₂ Batteries. *Nat. Energy* **2016**, *1*, 16066.

(32) Landa-Medrano, I.; Lozano, I.; Ortiz-Vitoriano, N.; Ruiz de Larramendi, I.; Rojo, T. Redox Mediators: A Shuttle to Efficacy in Metal–O₂ Batteries. *J. Mater. Chem. A* **2019**, *7*, 8746–8764.

(33) Lacey, M. J.; Frith, J. T.; Owen, J. R. A Redox Shuttle to Facilitate Oxygen Reduction in the Lithium Air Battery. *Electrochem. Commun.* **2013**, *26*, 74–76.

(34) Matsuda, S.; Hashimoto, K.; Nakanishi, S. Efficient Li₂O₂ Formation via Aprotic Oxygen Reduction Reaction Mediated by Quinone Derivatives. *J. Phys. Chem. C* **2014**, *118*, 18397–18400.

(35) Tesio, A. Y.; Blasi, D.; Olivares-Marín, M.; Ratera, I.; Tonti, D.; Veciana, J. Organic Radicals for the Enhancement of Oxygen Reduction Reaction in Li–O₂ Batteries. *Chem. Commun.* **2015**, *51*, 17623–17626.

(36) Gao, X.; Chen, Y.; Johnson, L.; Bruce, P. G. Promoting Solution Phase Discharge in Li–O₂ Batteries Containing Weakly Solvating Electrolyte Solutions. *Nat. Mater.* **2016**, *15*, 882–888.

(37) Chen, Y.; Freunberger, S. A.; Peng, Z.; Fontaine, O.; Bruce, P. G. Charging a Li–O₂ Battery Using a Redox Mediator. *Nat. Chem.* **2013**, *5*, 489–494.

(38) Sun, D.; Shen, Y.; Zhang, W.; Yu, L.; Yi, Z.; Yin, W.; Wang, D.; Huang, Y.; Wang, J.; Wang, D.; Goodenough, J. B. A Solution-Phase Bifunctional Catalyst for Lithium–Oxygen Batteries. *J. Am. Chem. Soc.* **2014**, *136*, 8941–8946.

(39) Kwak, W.-J.; Hirshberg, D.; Sharon, D.; Shin, H.-J.; Afri, M.; Park, J.-B.; Garsuch, A.; Chesneau, F. F.; Frimer, A. A.; Aurbach, D.; Sun, Y.-K. Understanding the Behavior of Li–Oxygen Cells Containing LiI. *J. Mater. Chem. A* **2015**, *3*, 8855–8864.

(40) Landa-Medrano, I.; Olivares-Marín, M.; Bergner, B.; Pinedo, R.; Sorrentino, A.; Pereiro, E.; Ruiz de Larramendi, I.; Janek, J.; Rojo, T.; Tonti, D. Potassium Salts as Electrolyte Additives in Lithium–Oxygen Batteries. *J. Phys. Chem. C* **2017**, *121*, 3822–3829.

(41) Chen, Y.; Gao, X.; Johnson, L. R.; Bruce, P. G. Kinetics of Lithium Peroxide Oxidation by Redox Mediators and Consequences for the Lithium–Oxygen Cell. *Nat. Commun.* **2018**, *9*, 767.

(42) Kwak, W.-J.; Park, J.; Kim, H.; Joo, J. M.; Aurbach, D.; Byon, H. R.; Sun, Y.-K. Oxidation Stability of Organic Redox Mediators as Mobile Catalysts in Lithium–Oxygen Batteries. *ACS Energy Lett.* **2020**, *5*, 2122–2129.

(43) Licini, G.; Mba, M.; Zonta, C. Amine Triphenolate Complexes: Synthesis, Structure and Catalytic Activity. *J. Chem. Soc., Dalton Trans.* **2009**, 5265.

(44) Bernardinelli, G.; Seidel, T. M.; Kündig, E. P.; Prins, L. J.; Kolarovic, A.; Mba, M.; Pontini, M.; Licini, G. Stereoselective Dimerization of Racemic C₃-Symmetric Ti(IV) Amine Triphenolate Complexes. *Dalton Trans.* **2007**, 1573–1576.

(45) Miceli, C.; Rintjema, J.; Martin, E.; Escudero-Adán, E. C.; Zonta, C.; Licini, G.; Kleij, A. W. Vanadium(V) Catalysts with High Activity for the Coupling of Epoxides and CO₂: Characterization of a Putative Catalytic Intermediate. *ACS Catal.* **2017**, *7*, 2367.

(46) Amadio, E.; González-Fabra, J.; Carraro, D.; Denis, W.; Gjoka, B.; Zonta, C.; Bartik, K.; Cavani, F.; Solmi, S.; Bo, C.; Licini, G. Efficient Vanadium-Catalyzed Aerobic C–C Bond Oxidative Cleavage of Vicinal Diols. *Adv. Synth. Catal.* **2018**, *360*, 3286.

(47) Badetti, E.; Gjoka, B.; Nagy, E. M.; Bernardinelli, G.; Kündig, E. P.; Zonta, C.; Licini, G. Mononuclear Iron(III) Complexes as Functional Models of Catechol Oxidases and Catalases. *Eur. J. Inorg. Chem.* **2015**, 3478.

(48) Mba, M.; Pontini, M.; Lovat, S.; Zonta, C.; Bernardinelli, G.; Kündig, E. P.; Licini, G. C₃Vanadium(V) Amine Triphenolate Complexes: Vanadium Haloperoxidase Structural and Functional Models. *Inorg. Chem.* **2008**, *47*, 8616.

(49) Badetti, E.; Lloveras, V.; Romano, F.; Di Lorenzo, R.; Veciana, J.; Vidal-Gancedo, J.; Zonta, C.; Licini, G. Discrimination of Octahedral versus Trigonal Bipyramidal Coordination Geometries of Homogeneous Ti(IV), V(V), and Mo(VI) Amino Triphenolate Complexes through Nitroxyl Radical Units. *Eur. J. Inorg. Chem.* **2016**, 4968.

(50) Zardi, P.; Wurst, K.; Licini, G.; Zonta, C. Concentration-Independent Stereodynamic g-Probe for Chiroptical Enantiomeric Excess Determination. *J. Am. Chem. Soc.* **2017**, *139*, 15616–15619.

(51) Zonta, C.; Kolarovic, A.; Mba, M.; Pontini, M.; Kündig, E. P.; Licini, G. Enantiopure Ti(IV) Amino Triphenolate Complexes as NMR Chiral Solvating Agents. *Chirality* **2011**, *23*, 796.

(52) Bravin, C.; Badetti, E.; Scaramuzzo, F. A.; Licini, G.; Zonta, C. Triggering Assembly and Disassembly of a Supramolecular Cage. *J. Am. Chem. Soc.* **2017**, *139*, 6456.

(53) Bravin, C.; Licini, G.; Hunter, C. A.; Zonta, C. Supramolecular Cage Encapsulation as a Versatile Tool for the Experimental Quantification of Aromatic Stacking Interactions. *Chem. Sci.* **2019**, *10* (). DOI: DOI: 10.1039/c8sc04406f.

(54) Bravin, C.; Licini, G.; Hunter, C. A.; Zonta, C. Hetero Co-Encapsulation within a Supramolecular Cage. Moving Away from the Statistical Distribution of Different Guests. *Chem.—Eur. J.* **2020**, *26*, n/a (/a). DOI: DOI: 10.1002/chem.202000574.

(55) Kulikov, A. V.; Likhtenstein, G. I. The Use of Spin Relaxation Phenomena in the Investigation of the Structure of Model and Biological Systems by the Method of Spin Labels. *Adv. Mol. Relax. Interact. Process.* **1977**, *10*, 47–79.

(56) Lloveras, V.; Liko, F.; Pinto, L. F.; Muñoz-Gómez, J. L.; Veciana, J.; Vidal-Gancedo, J. Tuning Spin-Spin Interactions in Radical Dendrimers. *ChemPhysChem* **2018**, *19*, 1895–1902.